6. Neybor, PNI, No. 4, 113 (1966).
7. Low-Temperature Calorimetery [Russian translation], Mir (1971).
8. Moses, Ben-Aroya, and Lupu, PNI, No. 8, 161 (1977).
9. Bachman et al., PNI, No. 2, 21 (1972).
10. V. N. Naumov and V. V. Nogteva, Seventh All-Union Conference on Calorimetry (Expanded Summaries of Reports) [in Russian], Moscow (1977), p. 488.
11. V. N. Naumov, V. V. Nogteva, and I. E. Paukov, Zh. Fiz. Khim., 53, 497 (1979).
12. P. F. Sullivan and G. Seidel, Phys. Rev., 173, 679 (1968).
13. Fagaly and Bon, PNI, No. 11, 143 (1977).

INVESTIGATION OF 10.6 μ ABSORPTION COEFFICIENT FOR CARBON DIOXIDE MOLECULES AT TEMPERATURES UP TO 3500°K

I. E. Zabelinskii, N. A. Fomin, and O. P. Shatalov

UDC 621.378.33

Experimental data are used to analyze features of resonance absorption processes in the high-temperature region, where the influence of hot transitions is appreciable.

At present a considerable amount of information has accumulated on the behavior of the absorption coefficient at low and intermediate temperatures. By measuring the 10.6 μ radiation absorption coefficient in test cells, investigators have studied the $\alpha(T)$ relationship up to temperatures of ∿650°K [1-6]. The development of gasdynamic lasers [7] has led to a need to analyze absorption processes at higher temperatures. These investigations were conducted using the region behind the front of a shock wave in shock tubes as the absorbing cell: in [8] absorption coefficient data were obtained up to temperatures of ∿1600°K, and in [9, 10] measurements were made up to ∿ 2100°K.

Meanwhile, absorption of 10.6 μ radiation by CO_2 molecules at higher temperatures is scientific interest, e.g., in analyzing recombination processes, in investigating spectral processes in dense gases, and also in investigation of the characteristics of high-temperature gasdynamic lasers [11].

The present paper uses experimental data on the resonance absorption in carbon dioxide at high temperatures, obtained in a large-diameter shock tube (the VUT-1 facility at the Institute of Mechanics, M. V. Lomonosov Moscow State University), to discuss features of the absorption process in the high-temperature region (up to 3500°K).

Description of the Facility. The experiments were conducted in a shock tube of internal diameter 493 mm (see, e.g., [12]). The radiative absorption was investigated behind the incident shock front in pure CO_2 and in CO_2 + Ar mixtures. Argon of special purity (99.98%) and specially dried carbon dioxide gas (the drying agent was P_2O_5) were used. The shock tube was pumped down to $2 \cdot 10^{-2}$ torr. The rate of inflow of air due to imperfect sealing of the shock tube and desorption of gas from the walls did not exceed 10^{-3} torr/min.

The gas mixture was made up in a special mixer, and was mixed beforehand (by a fan mounted inside the mixer) for several minutes prior to each shock tube filling. The pressure in the shock tube after filling with gas was measured with an oil manometer to an accuracy of better than 1%. The initial pressure was 3-60 torr. The shock wave speed was measured from the signals of piezoelectric sensors (located along the shock tube section) to an accuracy of better than 2%. Radiation from a type GL-23 laser, modulated by a mechanical shutter, passed through the shock tube via a BaF_2 window and fell on a semiconductor detector (germanium, doped with gold), from which the signal was recorded on an oscilloscope. At the same time, part of the laser radiation was directed to an infrared monochromator via a semitransparent

Institute of Mechanics, M. V. Lomonosov Moscow State University, Moscow. A. V. Lykov Institute of Heat and Mass Transfer, Academy of Sciences of the Belorussian SSR, Minsk. Translated from Inzhenerno-Fizicheskii Zhurnal, Vol. 37, No. 6, pp. 1074-1082, December, 1979. Original article submitted November 21, 1978.

0022-0841/79/3706-1461$07.50

TABLE 1. Experimental Data

Composition	J	T °K	P, atm	α_{exp}, m^{-1}	α_{calc}, m^{-1}
CO_2+4Ar	26	1250	0,7	0,4	1,34
CO_2+Ar	22	1260	1,34	0,12	1,125
CO_2	24	1200	0,63	1,86	1,86
CO_2+4Ar	26	1560	0,95	0,45	1,18
CO_2	24	1480	1,82	1,01	1,01
CO_2	12	1960	0,84	0,5	0,5
CO_2	26	2030	0,7	0,63	0,63
CO_2+9Ar	22	1930	0,37	0,25	0,88
CO_2	26	2110	0,73	0,93	0,93
CO_2	20	2220	1,66	0,429	0,429
CO_2	26	2730	0,6	0,838	0,838
CO_2+9Ar	22	3200	0,88	0,129	0,81
CO_2+9Ar	24	3440	0,73	0,126	0,784

mirror, which allowed simultaneous monitoring of the wavelength generated by the laser, using the semiconductor detector, during the experiment. In most of the experiments lasing was observed in the P branch laser transition with rotational quantum numbers J from 20 to 26.

In front of the entrance window of the semiconductor detector there was a 10.6 μ interference filter to suppress the gas self-radiation from the shock tube. Control experiments were conducted to check that the detectors did not record any signals when the shock wave passed through the measuring section with no laser radiation present.

Reduction of the Experimental Results. At low values of gas temperature behind the shock front (in the absence of dissociation) the oscillograms were analyzed for the equilibrium flow region, which was clearly observed at some distance from the shock front. At high temperatures and in the mixtures with argon, because of the excitation of oscillations, there was dissociation of CO_2 molecules, which appeared on the oscillogram as a characteristic maximum followed by a drop in the absorption coefficient.

In this case the absorption coefficient was measured at the maximum. The gas parameters at this point (temperature and pressure) were calculated from the conservation laws, based on the initial experimental parameters — pressure, composition, room temperature — and the measured shock speed, assuming that the vibrational relaxation of the CO_2 molecules is complete and that there is no dissociation. This assumption, that the relaxation and dissociation zones for CO_2 are separated, is valid in the temperature range investigated (see, e.g., [13]). The main results of the experiment are shown in Table 1. Since, as can be seen from the data of Table 1, several parameters were varied simultaneously during the experiments along with the gas temperature (the gas composition and pressure, and the rotational quantum number of the probe laser), Table 1 shows calculated values of absorption coefficient corresponding to 100% CO_2, P_2 = 1 atm, and J = 20 in addition to the measured values. The calculation allowed for the influence of hot transitions.

Theoretical Description of the Absorption Coefficients. The complexity of a theoretical description of the coefficient for absorption of the 10.6 μ radiation at high temperature stems from the need to allow for the contribution of hot transitions to the absorption process. It turns out that the frequencies of a transition series of the type $(n, m^l, p) \to (n-1, m^l, p+1)$ lie quite close to the frequency of the main absorption transition $(10^00) \to (00^01)$. At the same time, at temperatures $\geqslant$800°K the high levels of the CO_2 molecule become populated.

We can evaluate the number of transitions for which the difference in populations constitutes, e.g., 1% or more of the difference in populations for the basic transition:

$$\frac{\Delta N\,[(n,\ m^l,\ p)\to(n-1,\ m^l,\ p+1)]}{\Delta N\,[(10^00)\to(00^01)]}\simeq \exp-\left[\frac{(n-1)\,\Theta_1+m\Theta_2+p\Theta_3}{T}\right]\geqslant 10^{-2}.$$

We obtain the result that

$$(n-1)\,\Theta_1+m\Theta_2+p\Theta_3\leqslant 4.6\,T. \tag{1}$$

Here Θ_1, Θ_2, Θ_3 are characteristic temperatures for the symmetric, deformed, and asymmetric quanta of the CO_2 molecule. It is easy to see from the ratio obtained that there are 10 such transitions at T = 1000°K. With increase of temperature up to 3000°K the number of transitions goes up to 392.

TABLE 2. Basic Spectroscopic Constants for the Calculated Transitions

Transition	Type of symmetry	J'	E', cm^{-1}	B', cm^{-1}	$D' \cdot 10^7$, cm^{-1}
$10^00 \to 00^01$	$\Sigma_g^+ \to \Sigma_u^+$	Even	1388,186	0,390189	1,150
$11^10 \to 01^11$	$\Pi_u \to \Pi_{g,d-d}$	Even	2076,865	0,391344	1,195
$11^10 \to 01^11$	$\Pi_u \to \Pi_{g,c-c}$	Even	2076,865	0,390416	1,281
$12^00 \to 02^01$	$\Sigma_g^+ \to \Sigma_u^+$	Even	2671,113	0,389556	1,331
$10^01 \to 00^02$	$\Sigma_u^+ \to \Sigma_g^+$	Even	3714,781	0,387063	1,137
$10^02 \to 00^03$	$\Sigma_g^+ \to \Sigma_u^+$	Even	6016,690	0,383917	1,170
$10^03 \to 00^04$	$\Sigma_u^+ \to \Sigma_g^+$	Even	8293,957	0,380805	1,130

Transition	Type of symmetry	E'', cm^{-1}	B'', cm^{-1}	$D'' \cdot 10^7$, cm^{-1}	$\left[\frac{R}{R_{10^00 \to 00^01}}\right]^2$
$10^00 \to 00^01$	$\Sigma_g^+ \to \Sigma_u^+$	2349,164	0,387141	1,330	1,00
$11^10 \to 01^11$	$\Pi_u \to \Pi_{g,d-d}$	3004,016	0,388190	1,349	0,95
$11^10 \to 01^11$	$\Pi_u \to \Pi_{g,c-c}$	3004,016	0,387593	1,349	0,95
$12^00 \to 02^01$	$\Sigma_g^+ \to \Sigma_u^+$	3612,844	0,387504	1,580	1,19
$10^01 \to 00^02$	$\Sigma_u^+ \to \Sigma_g^+$	4673,327	0,384066	1,326	2,32
$10^02 \to 00^03$	$\Sigma_g^+ \to \Sigma_u^+$	6972,578	0,380990	1,331	4,01
$10^03 \to 00^04$	$\Sigma_u^+ \to \Sigma_g^+$	9246,805	0,377900	1,130	6,12

In this estimate we accounted only for the ratio of populations. In actual fact, the influence of hot transitions will be considerably less because of the inexact coincidence of the centers of transition lines. Nevertheless, for an accurate calculation we must know the Einstein coefficients, the cross sections for collision line broadening, and the positions of the centers of the transition lines, taking into account the rotational structure for each computed transition.

Einstein Coefficients. Analysis of the experimental data on the Einstein coefficients for the P20 line of the main (10°0) → (00°1) transition made in [14] led those authors to recommend a most probable value of $A_{21} = 0.187$ sec^{-1}. The dependence on the sublevel rotational number can be established by expressing the value A_{21} in terms of the square of the matrix element for the dipole moment of the vibrational transitions $(R_{V'V''})^2$ (the quantity $(R_{V'V''})^2$ does not depend on the number J) [15]:

$$A_{21} = \frac{1}{g_2} \frac{64\pi^4 \nu_0^3}{3hc^3} S(J) (R_{V'V''})^2.$$

Here S(J) is the Hönl—London factor, which is equal to J for the P branch and to J + 1 for the R branch with good accuracy.

Since we have no experimental data on the Einstein coefficients for the hot transitions we used calculated values for the squares of the matrix elements of the transition dipole moments, as shown in Table 2, from the data of [16].

Spectral Line Broadening. To describe the shape of a spectral line, one uses the Voigt profile

$$\alpha(\nu, a) = \alpha_0 \frac{\sqrt{\ln 2}}{\Delta\nu_D} \frac{a}{\pi} \int_{-\infty}^{\infty} \frac{\exp(-y^2)\, dy}{a^2 + (x - y)^2},$$

where α_0 is the absorption coefficient at the line center, and $x = (\nu - \nu_0)\sqrt{\ln 2}/\Delta\nu_D$, $a = \Delta\nu_C\sqrt{\ln 2}/\Delta\nu_D$ ($\Delta\nu_C$, $\Delta\nu_D$ are the Lorentz and the Doppler half-widths of the profile). In addition, it is assumed that the collisional half-width is $\Delta\nu_C \sim 1/T$ [9, 10].

The broadening constants for collisions with CO_2 and Ar were assumed to be 0.096 $cm^{-1} \cdot atm^{-1}$ and 0.055 $cm^{-1} atm^{-1}$, respectively. The cross section for absorption line broadening varies very little with variation of rotational line number. As was shown in [18, 19], the dependence for the CO_2 molecule may be approximated as follows:

$$\sigma(J) = \sigma_0 - 0.0008 (J \pm 1),$$

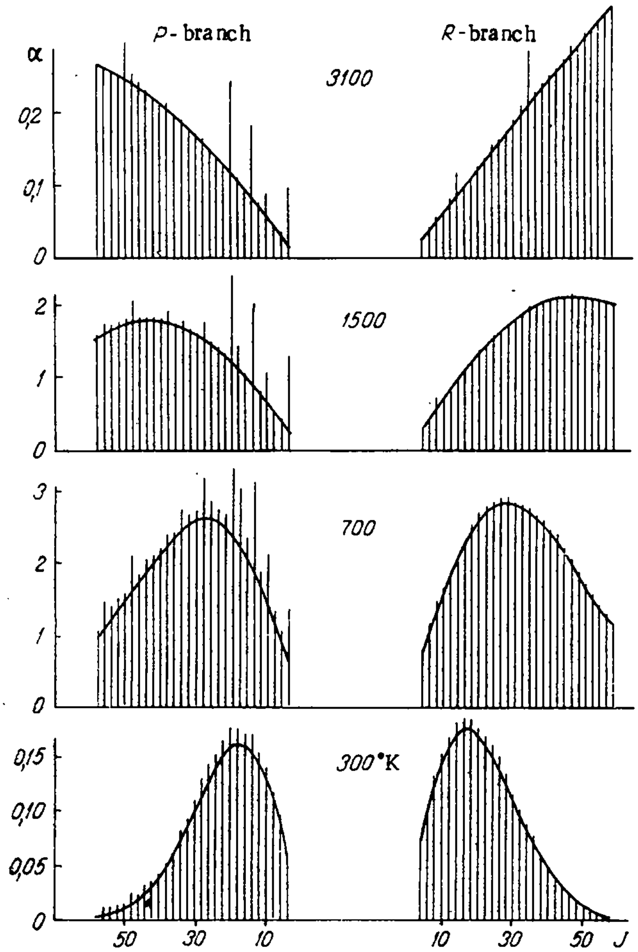

Fig. 1. Spectral distributions (dependence on the number J of the probe laser) of the resonance absorption coefficient in the 10.6 μ region (the 10°0 → 00°1 transition) for various temperatures of carbon dioxide gas (calculated). The pressure is 2 atm, and α is in m^{-1}.

where the "plus" sign refers to the P branch and the "minus" sign refers to the R branch transition.

It was shown in [17] that the cross sections for broadening for hot transitions are equal to the corresponding cross sections for the main transition to within 5%. The Doppler half-width was calculated from the standard relations [7].

Positions of the Line Centers. Until recently the lack of precision in determining the position of transition line centers was considerable, and, e.g., according to the data of [19, 20] was about 10^{-1} to 10^{-2} cm^{-1}. At the same time, in calculating the contribution of the hot transitions to the absorption coefficient, the uncertainty in the center of the transition line of 10^{-3} cm^{-1} leads to an error of about 4% (the estimate was made for a pressure of 1 atm and a temperature of 3000°K). The error decreases with increase in pressure or reduction in temperature. However, recently a number of laboratories have made precision measurements (to an accuracy of 10^{-5} cm^{-1} or better of the line center positions [20-24]. The results have been correlated in [25, 26], and one can now calculate the positions of the centers of the spectral lines with sufficient accuracy from the following relations:

$$E_i = E_0 + B_i[J(J+1) - l^2] - D_i[J(J+1) - l^2]^2 + H_i[J(J+1) - l^2]^3 - L_i[J(J+1) - l^2]^4,$$
$$E(P\ \text{branch}) = E_2(J-1) - E_1(J),$$
$$E(R\ \text{branch}) = E_2(J+1) - E_1(J).$$

Here E_0 is the center of the vibrational transition, the subscript 1 refers to the lower state, and 2 refers to the upper state. The values of E_0, B_i, and D_i for the most important transitions are shown in Table 2, and a number of other constants required are given in [25, 26].

Discussion of Results. The dependence of the absorption coefficient for the 10°0 → 00°1 transition (wavelength 10.6 μ) on the basic parameters is shown in Figs. 1-3. Figure 1 shows the calculated data on the spectral distribution of the absorption coefficient (dependence on the probe laser number J) in the P and R branches for various values of the medium temperature. The solid curves in the figures correspond to the Boltzmann distribution of rota-

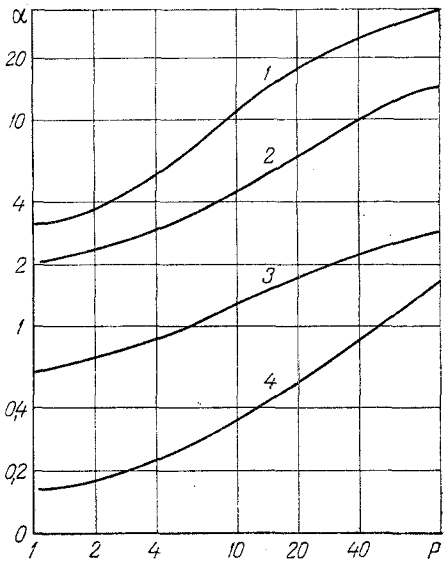

Fig. 2

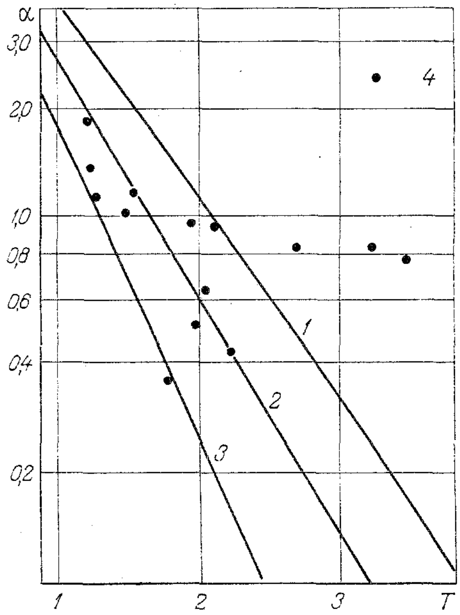

Fig. 3

Fig. 2. Calculated dependence of the absorption coefficient at the P20 line on pressure. The gas temperature is: 1) T = 700°K; 2) 1500°K; 3) 2500°K; 4) T = 300°K. α, m^{-1}; P, atm.

Fig. 3. Calculated (1-3) and experimental (4) data on the temperature dependence of the absorption coefficient. The pressure is 1 atm; 1, 3) the P20 line; 2) the P18 line. Curves 2 were constructed under the assumption that $\Delta\nu_c \sim 1/T$, and curve 3 was constructed under the assumption that $\Delta\nu_c \sim 1/\sqrt{T}$), α, m^{-1}; T, 10^3°K.

tional sublevels, without allowing for the effects of overlap and the contribution of the hot transitions. Analysis of the results of the calculations shows that for low pressures ($P \leqslant 0.1$ atm) the distribution of the absorption coefficient over the rotational sublevels is of Boltzmann type.

This is exactly the circumstance that allows us to conduct diagnostic measurements of gas flows (to determine the rotational temperature and therefore also the vibrational temperature) at low pressures, e.g., of nonequilibrium flows in gasdynamic lasers. For pressures increased above atmospheric the situation is more complex. For example, in Fig. 1 the spectral distributions correspond to a pressure of 2 atm. It can be seen that for T = 300°K the actual distribution differs insignificantly from a Boltzmann distribution. At higher temperatures ($T \geqslant 500$-700°K) there is a considerable increase in the absorption coefficient only for those lines which have resonance coincidence with the hot transition lines. In particular, in Fig. 1 one can see an anomalous behavior of the P20 line, due to a good resonance with the R23 line of the $11^10 \to 01^11$ transition. With further temperature increase there is excitation of all the higher transitions and new "rejects" appear in the absorption spectrum, corresponding to resonances with the hotter transitions; but one must bear in mind that the half-width of the absorption line ($\Delta\nu_c \sim 1/T$) decreases for increased temperature and therefore the overlap effects diminish.

The nature of the variation of the absorption coefficient with pressure is illustrated by the relations shown in Fig. 2. It can be seen that the rate of growth of the absorption coefficient with pressure is different for different temperature regions: at low gas temperatures ($T \approx 300$°K) it is due mainly to overlap of the rotational sublevels of the main transition, and for higher temperatures ($T \approx 1000$-3000°K), when the populations of the hot transitions are considerable, the increase of α is due mainly to the effects of overlap with individual lines of the hot transitions.

Figure 3 shows the results of calculating the temperature dependence of this parameter and compares these results with the experimental data. It can be noted that, in the temperature region up to 2100°K, the measured results in Fig. 3 correlate very well with the data of [9]; at temperatures above 2100°K, the experimental data on the absorption coefficient were obtained for the first time. Comparison of the experimental relations with those calculated indicates that up to temperatures of $\sim$2500°K the value of α can be determined from the above relations, allowing for the effects of overlap and bringing in the relation $\Delta\nu_c \sim 1/T$. It can be seen that the calculated values obtained from the assumption that $\Delta\nu_c \sim \sqrt{1/T}$ differ considerably, even for $T \geqslant 1000$°K, from the experimental data.

For temperatures above 2500°K one sees a considerable increase in the experimental data over the calculated values even for the assumed relation $\Delta\nu_c \sim 1/T$. The reasons for this discrepancy are not well understood, but one should note that a similar picture is observed in describing the dependence of the absorption coefficient on the pressure for $P \geqslant 10$ atm even at room temperature: the experimental data lie appreciably above the calculated values. In describing the absorption line profile width under conditions of strongly overlapping lines we have rejected the Lorentz relations. Miller [27, 28] was able to describe quantitatively the dependence of the amplification factor at high pressures. In addition, in the experimental conditions in the shock tube behind strong shock waves, considerable irregularities and turbulence of the medium may arise, which can also bring in additional losses in the measurement of the absorption coefficient at high temperatures.

In conclusion the authors thank R. I. Soloukhin and S. A. Losev for numerous useful discussions and suggestions. The authors also thank I. F. Golovnev for calculating the matrix elements of the dipole moments of the hot transitions, and also J. Dupre-Maquaire, P. Pinson, J. Manden, J. Reid, and K. Simpson, who made available the results of their spectroscopic investigations of the CO_2 molecule.

NOTATION

α, absorption coefficient; T, gas temperature; J, rotational quantum number; n, m, l, p, vibrational quantum numbers; Θ_i, characteristic temperature of the i-th mode; ΔN, inversion; A_{21}, Einstein coefficient; $(R_{V'V''})^2$, square of the transition dipole moment matrix element; S(J), Hönl-London factor; ν, transition frequency; c, speed of light; g_i, statistical weight of state i; $\Delta\nu_c$, $\Delta\nu_D$, collisional (Lorentz) and Doppler half-widths; σ, cross section for optical broadening; E, level frequency; B, D, H, L, rotational constants; P, pressure.

LITERATURE CITED

1. E. T. Gerry and D. A. Leonard, Appl. Phys. Lett., 8, No. 9 (1966).
2. T. K. McCubbin, Jr., R. Darone, and J. Sorrell, Appl. Phys. Lett., 8, No. 5 (1966).
3. T. K. McCubbin, Jr., and T. R. Mooney, JQRTS, 8, No. 5, 1255 (1968).
4. R. L. Leonard, Appl. Opt., 13, No. 8, 1920 (1974).
5. S. A. Munjee and W. H. Christiansen, Appl. Opt., 12, No. 5, 993 (1973).
6. A. M. Robinson and N. Sutton, Appl. Opt., 16, No. 10, 2632 (1977).
7. S. A. Losev, Gasdynamic Lasers [in Russian], Nauka, Moscow (1977).
8. A. R. Strilchuk and A. A. Offenberger, Appl. Opt., 13, No. 11, 2643 (1974).
9. R. I. Soloukhin and N. A. Fomin, Zh. Prikl. Mekh. Tekh. Fiz., No. 1 (1977).
10. N. A. Fomin, Author's Abstract of Candidate's Dissertation, ITMO, Akad. Nauk BSSR, Minsk (1978).
11. R. I. Soloukhin, "The shock tube in flow laser research: modeling and applications," in: Proceedings of the Eleventh International Shock Tube Symposium, B. Alborn, A. Herzbert, and D. Russell (eds.), Washington Univ. Press (1978).
12. S. A. Losev, V. N. Makarov, V. A. Pavlov, and O. P. Shatalov, Fiz. Goreniya Vzryva, 9, No. 4 (1973).
13. E. V. Stupochenko, S. A. Losev, and A. I. Osipov, Relaxation Processes in Shock Tubes [in Russian], Nauka, Moscow (1965).
14. A. S. Biryukov, A. Yu. Volkov, E. M. Kudyryavtsev, and R. I. Serikov, Kvant. Élektron., 3, No. 8 (1976).
15. S. S. Penner, Quantitative Molecular Spectroscopy and Gas Emissivities, Addison-Wesley (1959).
16. I. F. Golovnev (Golovnyov), V. G. Sevast'yanenko, and R. I. Soloukhin, J. Eng. Phys., 26, No. 2 (1979).
17. J. Reid, J. Shewchun, and B. K. Garside, J. Appl. Phys., 17, 349 (1978).
18. N. G. Chang and M. T. Tavis, IEEE J. Quantum Electron., 10, No. 3, 372 (1974).
19. C. P. Courtoy, Can. J. Phys., 35, No. 5, 608 (1957).

20. D. M. Dennison, Rev. Mod. Phys., 12, 175 (1940).
21. J.-P. Moncilalin et al., J. Mol. Spectrosc., 63, 491 (1977).
22. J. Dupre-Maquaire and P. Pinson, J. Mol. Spectrosc., 62, 181 (1976).
23. D. Bailly, R. Farreng, and C. Rossetty, J. Mol. Spectrosc., 70, 124 (1978).
24. D. A. Steinor et al., J. Mol. Spectrosc., 64, 438 (1977).
25. R. A. McClatchey et al., Air Force Cambridge Research Lab. Rep., AFCRL-TR-73-0096 (1973).
26. L. S. Rothman and W. S. Benedict, Appl. Opt., 17, No. 16, 2605 (1978).
27. J. L. Miller and E. V. George, Appl. Phys. Lett., 27, 665 (1975).
28. J. L. Miller, J. Appl. Phys., 49, No. 6, 3076 (1978).

DIFFUSIOPHORESIS OF LIQUID DROPS IN VISCOUS MEDIA WITH DUE CONSIDERATION OF INTERNAL FLOWS AND THE PHASE TRANSITION ON THEIR SURFACE

Yu. M. Agvanyan and Yu. I. Yalamov

UDC 541.182:532.72

A theory of diffusiophoresis of a spherical drop in a binary viscous mixture with nonuniform concentration is developed.

In construction of a theory of motion of liquid drops in viscous media with a phase transition occurring on their surface internal flows have not been taken into account so far [1-9]. In fact, drops whose viscosity is very much greater than the viscosity of the external medium surrounding them have been considered. In these conditions the presence of hydrodynamic flows inside the drop can be neglected.

It was shown in [10-12] by the examples of gravitational, thermophoretic, and diffusiophoretic motion of nonvolatile drops in viscous media that the contribution of internal flows to the velocity becomes very substantial if the viscosity of the internal region of the drop is comparable with the viscosity of the medium surrounding the drop. It has also been found that with increase in the radius of the nonvolatile drops of water their velocity of thermophoresis in gases (particularly in air) will depend significantly on the interphase surface tension, which varies over the surface of the drops [11].

Throughout the paper the term "nonvolatile drop" means a drop on whose surface there is no phase transition of the substance of which it consists. The term "volatile drop" means a drop on whose surface there is a phase transition of the substance of which it consists.

In this paper we consider the diffusiophoresis of a large volatile spherical drop of radius R in a binary viscous mixture. By a viscous mixture we mean either a gaseous or liquid mixture. Far from the drop gradients of the relative concentrations $(\nabla C_{1e})_\infty$ and $(\nabla C_{2e})_\infty$ of the mixture components are maintained in the volume of the medium. If the drop is surrounded by a binary gas mixture we choose as C_{1e} and C_{2e} the relative numerical concentrations of the molecules: $C_{1e} = n_{1e}/n_e$, $C_{2e} = n_{2e}/n_e$, $n_e = n_{1e} + n_{2e}$, n_{1e} and n_{2e} are the numbers of molecules of the first and second components of the mixture in unit volume. For the case of a liquid binary mixture external to the drop it is convenient to introduce relative mass concentrations C_{1e} and C_{2e} for the components:

$$C_{1e} = n_{1e}m_1/\rho_e \text{ and } C_{2e} = n_{2e}m_2/\rho_e,$$

where m_1 and m_2 are the masses of the molecules of the mixture components, and $\rho_e = n_{1e}m_1 + n_{2e}m_2$ is the density of the mixture.

The origin of the spherical system of coordinates r, θ, φ can be taken at the center of the drop. In this case the drop can be regarded as at rest, and the binary mixture as moving relative to the center of the drop at constant velocity **U**. If we choose $(\nabla C_{1e})_\infty$ along the polar axis $Z = r \cos \theta$, then vector **U** will be directed along this axis.

N. K. Krupskaya Moscow Regional Pedagogic Institute. Translated from Inzhenerno-Fizicheskii Zhurnal, Vol. 37, No. 6, pp. 1083-1088, December, 1979. Original article submitted March 19, 1979.

0022-0841/79/3706-1467$07.50